

引用格式: 万文鹏, 黄春杰, 许爱军, 等. 冷喷涂 Cr 涂层的组织性能与沉积机制[J]. 材料工程, 2026, 54(3): 229-235.
WAN Wenpeng, HUANG Chunjie, XU Aijun, et al. Microstructural characteristics and deposition mechanism of cold-sprayed Cr coatings[J]. Journal of Materials Engineering, 2026, 54(3): 229-235.

冷喷涂 Cr 涂层的组织性能与沉积机制

万文鹏^{1,2}, 黄春杰^{1,2*}, 许爱军³, 罗杰⁴, 王罗⁵, 傅硕^{1,2}, 徐雅欣^{1,2}, 李文亚^{1,2}

(1 西北工业大学 材料学院 凝固技术全国重点实验室, 西安 710072; 2 西北工业大学 材料学院 陕西省摩擦焊接工程技术重点实验室, 西安 710072; 3 长沙五七一二飞机工业有限责任公司, 长沙 410114;

4 苏州天河中电电力工程技术有限公司, 江苏 苏州 215027;

5 中广核工程有限公司 核电安全技术与装备全国重点实验室, 广东 深圳 518172)

摘要: 在 304 不锈钢基体上使用冷喷涂法和电镀法制备 Cr 涂层, 通过分析冷喷涂 Cr 涂层表面微观形貌、截面显微组织及纳米力学性能, 阐明 Cr 粉末颗粒的碰撞沉积行为及 Cr 涂层沉积机制。结果表明: 电镀 Cr 涂层存在大量纵向裂纹, 冷喷涂 Cr 涂层与基体之间的结合界面呈现不规则形态, 但界面结合紧密且无明显缺陷。同时, Cr 涂层表面存在大量凹坑, 且近表面区域表现为细小的等轴晶。该区域的纳米硬度较未变形 Cr 粉末颗粒提升了 41.37%~62.17%, 表明后续粉末颗粒在已沉积 Cr 涂层上产生由喷丸作用引起的加工硬化效应, 使后续粉末颗粒与已沉积涂层之间难以发生协同塑性变形, 从而降低了进一步沉积的可行性。基于 Cr 涂层微观形貌及梯度纳米硬度分布特征, 提出 Cr 涂层在 304 不锈钢上的沉积机制为基体氧化膜的破碎、首层涂层的形成及其在喷丸强化作用下表面微观形貌的演变过程。

关键词: 冷喷涂; Cr 涂层; 涂层成形机制; 微观组织; 纳米硬度

doi: 10.11868/j.issn.1001-4381.2025.000132 **CSTR:** 32421.14.j.issn.1001-4381.2025.000132

中图分类号: TG174.442; TB31 **文献标识码:** A **文章编号:** 1001-4381(2026)03-0229-07

Microstructural characteristics and deposition mechanism of cold-sprayed Cr coatings

WAN Wenpeng^{1,2}, HUANG Chunjie^{1,2*}, XU Aijun³, LUO Jie⁴, WANG Luo⁵,
FU Shuo^{1,2}, XU Yaxin^{1,2}, LI Wenya^{1,2}

(1 State Key Laboratory of Solidification Processing, School of Materials Science and Engineering, Northwestern Polytechnical University, Xi'an 710072, China; 2 Shaanxi Key Laboratory of Friction Welding Technologies, School of Materials Science and Engineering, Northwestern Polytechnical University, Xi'an 710072, China; 3 Changsha 5712 Aircraft Industry Co., Ltd., Changsha 410114, China; 4 Suzhou Tianhe China Power International Engineering Technology Co., Ltd., Suzhou 215027, Jiangsu, China; 5 State Key Laboratory of Nuclear Power Safety Technology and Equipment, China Nuclear Power Engineering Co., Ltd., Shenzhen 518172, Guangdong, China)

Abstract: The Cr coatings are fabricated on 304 stainless steel substrates using cold spray and electroplating methods. The particle deposition behavior and coating formation mechanism of Cr are clarified by analyzing the surface morphology, cross-sectional microstructure, and nanomechanical properties of the cold-sprayed Cr coatings. The results show that the electroplated Cr coating contains numerous vertical cracks, while the cold-sprayed Cr coating exhibits an irregular but compact and defect-free interface with the substrate. In addition, the surface of the cold-sprayed coating presents a large number of craters, and the near-surface region consists of fine equiaxed grains. The nanohardness in the region increases by 41.37%-62.17% compared with that of undeformed Cr particles, indicating that subsequent particles produce work hardening due to shot-peening effects upon impacting the pre-deposited coating. The hardening hinders cooperative plastic deformation between incoming particles and the existing coating, thereby reducing the feasibility of

further deposition. Based on the surface morphology and the gradient distribution of nanohardness, the deposition mechanism for Cr coatings on 304 stainless steel is proposed, involving the disruption of the substrate's oxide film, the formation of the initial coating layer, and the surface morphological evolution induced by shot-peening strengthening.

Key words: cold spraying; Cr coating; coating forming mechanism; microstructure; nanohardness

Cr因其优异的耐磨性、耐腐蚀性及高温抗氧化性,被广泛应用于金属表面防护涂层,以显著提升基体在高温、腐蚀等极端工况下的服役性能^[1-7]。目前, Cr涂层的工业化制备主要依赖传统电镀工艺^[8-9],然而该方法存在两大问题:(1)电镀过程中产生的纵向裂纹易成为应力集中源,导致涂层防护性能退化,无法长期保护基体^[10-13];(2)电镀液中的六价铬(Cr^{6+})具有强致癌性和环境不友好性,对人体健康以及自然环境均存在严重威胁。因此,开发绿色高效的Cr涂层替代制备技术成为当前表面工程领域的一个重要研究方向。近年来,等离子喷涂^[14-15]、物理气相沉积^[16-17]、超音速火焰喷涂^[18]以及激光熔敷^[19]等技术被尝试用于Cr涂层的制备。然而,等离子喷涂、超音速火焰喷涂与激光熔敷技术均涉及熔化-凝固或半熔化过程,易诱发涂层氧化及热应力积累,而物理气相沉积技术虽可制备高致密度涂层,但其低沉积速率与高成本严重制约了其在在大尺寸工业部件中的应用。冷喷涂技术作为一种新型固态沉积工艺,为解决上述问题提供了新的思路。该技术以高温、高压气体(如氮气、氦气或压缩空气)为载气,将微米级金属粉末(粒径 $15\sim 53\ \mu\text{m}$)经拉瓦尔喷嘴加速至 $300\sim 1200\ \text{m/s}$ 超音速状态后撞击基体^[20-23],粒子在固态下通过剧烈塑性变形实现机械咬合与冶金结合,其沉积温度低于材料熔点,从而有效抑制氧化及相变^[24-25]。相较于传统工艺,冷喷涂兼具高沉积速率、低热输入和环境友好等优势,已在航空部件修复与功能涂层制备领域展现出广阔的应用前景^[26]。

目前,冷喷涂Cr涂层的研究主要集中在铝合金基体,重点考察其在高温、高压及失水事故模拟工况下的耐腐蚀性、抗氧化性以及Cr涂层与铝合金基体之间的界面演变与元素扩散机制^[4,27-29]。然而,这些研究往往忽视了Cr粒子的沉积行为,而深入理解该过程对制备高质量涂层具有重要意义。此外,在其他工程材料上冷喷涂Cr涂层的研究尚属匮乏。针对这一不足,本工作选用典型工程材料304不锈钢为基体,通过对涂层表面和截面的微观组织演变及纳米硬度分布的系统分析,揭示Cr涂层在304不锈钢基体上的沉积机制,包括初始阶段Cr粒子与基体界面的相互作用,以及后续Cr粒子与已沉积涂层之间的动态演化过程。

1 实验材料与方法

1.1 实验材料

选用尺寸为 $100\ \text{mm}\times 50\ \text{mm}\times 3\ \text{mm}$ 的304不锈钢板材作为基体材料,所用Cr粉末(星尘科技(广东)有限公司提供)粒径为 $20\sim 62\ \mu\text{m}$,粉末粒径累积分布占比达到50%时对应的平均粒度 $D_{50}=44\ \mu\text{m}$ 。图1为Cr粉末的微观形貌,从图1(a)中可以发现,Cr粉末具有较高的球形度,少量粉末表面存在行星颗粒。图1(b)为图1(a)的局部放大图,可清晰观察到Cr粉末表面的胞状亚结构。

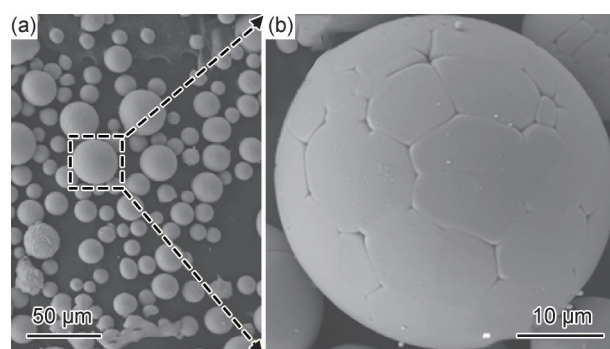


图1 Cr粉末微观形貌

(a)整体图;(b)局部放大图

Fig.1 Micromorphologies of Cr powder

(a)overall view;(b)local magnified view

1.2 冷喷涂Cr涂层的制备

在喷涂前,使用80目砂纸对304不锈钢基体表面进行打磨处理,以去除表面油污等污染物。随后,采用Impact 5/11商用喷涂系统(Impact Innovations公司)进行冷喷涂实验,喷嘴材料为WC,喷嘴的截面形状为收缩-扩张型,扩张比和下游长度分别为5.6和130 mm,喷涂过程中喷嘴与基体的距离为30 mm,喷枪的移动速度为 $200\ \text{mm/s}$,偏移量为2 mm,送粉器转速为 $4\ \text{r/min}$,送粉速率约为 $51.2\ \text{g/min}$,喷涂温度为 $1000\ ^\circ\text{C}$ 和 $1100\ ^\circ\text{C}$,喷涂压力为5 MPa,使用的工作气体和送粉气体均为氮气。

1.3 电镀Cr涂层的制备

在电镀前,使用丙酮对304不锈钢基体进行超声波清洗,清洗时间为5 min,随后使用吹风机将基体表

面吹干,电镀液的温度为60℃,电流密度为25 A/dm²,电镀时间为120 min。

1.4 表征方法

采用场发射扫描电子显微镜(SEM, Tescan Clara GMH)观察粉末形貌及涂层表面、截面形貌。涂层的电子背散射衍射(EBSD)分析在配备该装置的SEM设备上。在对涂层进行EBSD表征前,需对样品进行抛光处理,步骤如下:首先,将金相试样镶嵌后使用500~2000目砂纸进行研磨,随后依次使用粒径为3、1.5 μm和0.05 μm的金刚石悬浮液进行机械抛光,直至涂层表面无可见划痕,最后采用粒径为0.02 μm的二氧化硅悬浊液进行振动抛光,振幅为40%,抛光时间为8 h。

涂层及基体的纳米硬度通过纳米压痕仪(T1980)进行测试,涂层的纳米硬度在一个变形粒子内部进行4×4矩阵测量,为便于分析,靠近涂层/基体界面处至涂层表层的4列压痕点分别命名为Line 1、Line 2、Line 3和Line 4,共计16个压痕点,相邻点的距离为7 μm,覆盖整个涂层成形方向。

2 结果与分析

2.1 涂层微观形貌

图2为Cr涂层截面微观形貌。图2(a),(b)为使用冷喷涂法制备的Cr涂层,喷涂温度分别为1000℃和1100℃,图2(c)为通过电镀法制备的Cr涂层。结合图2(a),(b)可见,冷喷涂制备的Cr涂层与基体之间的结合界面呈不规则形态,原因为冷喷涂过程中不同粒径粒子与基体的碰撞速度有差异,导致粒子与基体之间的协同塑性变形程度不一致。此外,涂层与基体的结合界面未见微裂纹等缺陷,表明结合质量较好。冷喷涂温度的增加能够提升粒子的碰撞速度和温度,从而促进涂层厚度的增加^[30]。需要注意的是,当喷涂温度为1000℃时,涂层主要呈现单粒子沉积结构,厚度约为30 μm。后续粒子对已沉积Cr涂层的“喷丸效应”导致涂层表面发生加工硬化,从而无法继续沉积,尽管涂层内部存在少量颗粒间未结合界面,但整体呈现出较为致密的结构。当喷涂温度升高至1100℃时,涂层厚度增至约50 μm,但靠近涂层表面处出现较多微裂纹,表明在此喷涂温度下,后续Cr粒子可以在已沉积的Cr涂层上继续沉积,但其结合较为薄弱,结合质量较差。随着喷涂的进行,这些弱结合区域的Cr涂层可能会被后续Cr粒子冲蚀,从而限制了涂层厚度的进一步增加。综上所述,在这两种喷涂温度下,Cr粒子与基体之间能够有效结合,形成致密的首层Cr涂

层,但后续Cr粒子与已沉积涂层之间的结合效果较差。因此,为提高涂层的质量和厚度,需要进一步提升喷涂温度。从图2(c)中可以看出,电镀法制备的Cr涂层厚度约为100 μm,涂层与基体之间的界面较为平整。然而,涂层内部存在大量纵向微裂纹^[31],易引起应力集中,这不利于对基体的长期保护。通过上述对比可以发现,冷喷涂法制备的Cr涂层内部组织较为致密,且与基体的结合质量较好,展现出替代电镀的潜力。

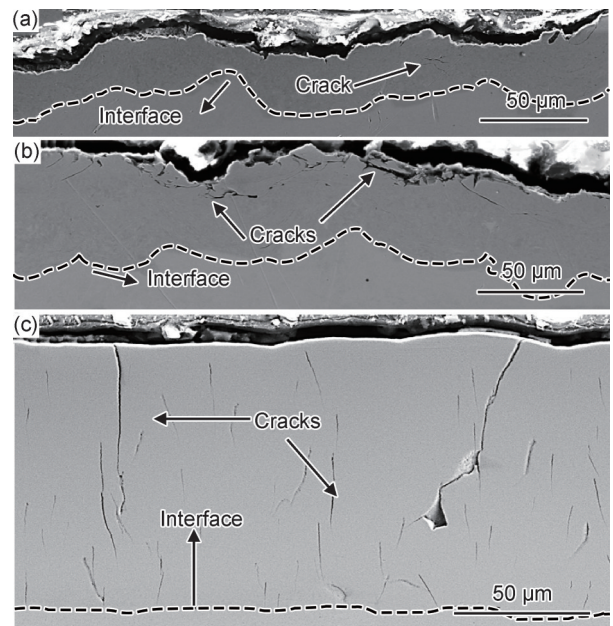


图2 Cr涂层截面微观形貌

(a)冷喷涂1000℃;(b)冷喷涂1100℃;(c)电镀

Fig.2 Microstructural morphologies of cross-sectional Cr coatings

(a) fabricated by cold spraying at 1000℃; (b) fabricated by cold spraying at 1100℃; (c) fabricated by electroplating

对涂层的表面形貌进行分析可在一定程度上判断冷喷涂过程中粒子的沉积行为。图3为不同喷涂温度下Cr涂层的表面微观形貌。可知两种喷涂温度所制备涂层的表面微观形貌类似,均存在大量凹陷,这与Wang等^[32]的发现一致。此外,还可以观察到个别粒子以嵌入的形式沉积在涂层表面,并且部分粒子存在开裂现象。这可能是由于粒子以极高的速度与涂层发生碰撞时,粒子的内聚强度不足从而发生破碎。结合图2和图3可知,当喷涂温度分别为1000℃和1100℃时,所得涂层的微观形貌未表现出显著差异。因此,本工作仅对1100℃喷涂温度下制备的Cr涂层截面进行EBSD分析,其结果如图4所示。从图4(a)可以观察到,涂层主要由两类晶粒组成:靠近基体一侧的晶粒呈拉长形态,而靠近涂层表面的区域则由细小等轴晶粒构成。图4(b)为涂层的晶粒取向差分布(grain orientation spread, GOS),可以发现涂层发生明

显的动态再结晶。图4(c)为晶界分布图,可知涂层内部主要由大角度晶界 (high-angle grain boundaries, HAGBs)组成。这一微观结构特征可归因于冷喷涂过程中后续粒子对涂层表面的持续撞击作用(即喷丸强化效应)。在此过程中,涂层表面经历剧烈的塑性变

形,伴随高密度位错的引入。这些位错在后续沉积过程中逐步重排,形成位错胞或亚晶界。随着塑性变形的累积,小角度晶界 (low-angle grain boundaries, LAGBs)在晶粒旋转作用下逐步转变为HAGBs,最终促使涂层表面形成细小等轴晶粒^[33]。

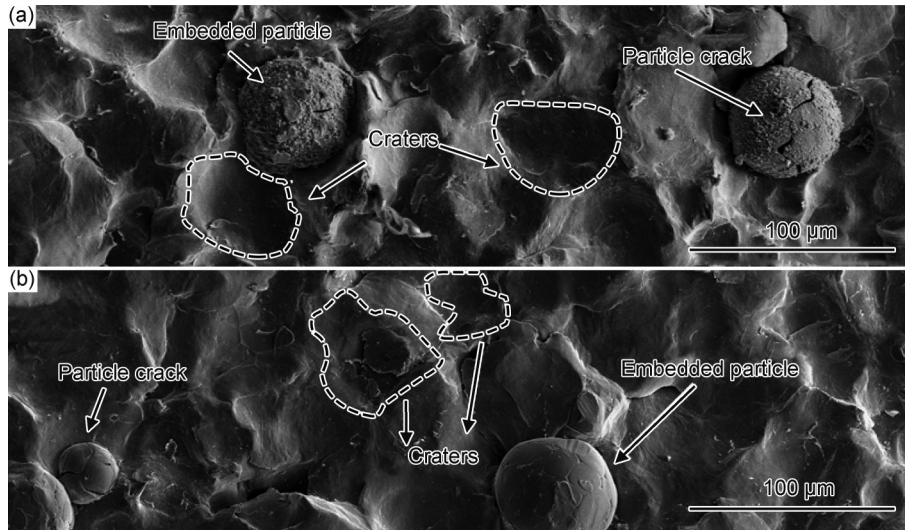


图3 不同喷涂温度下Cr涂层表面微观形貌 (a)1000 °C;(b)1100 °C

Fig.3 Surface morphologies of Cr coatings at different spraying temperatures (a)1000 °C;(b)1100 °C

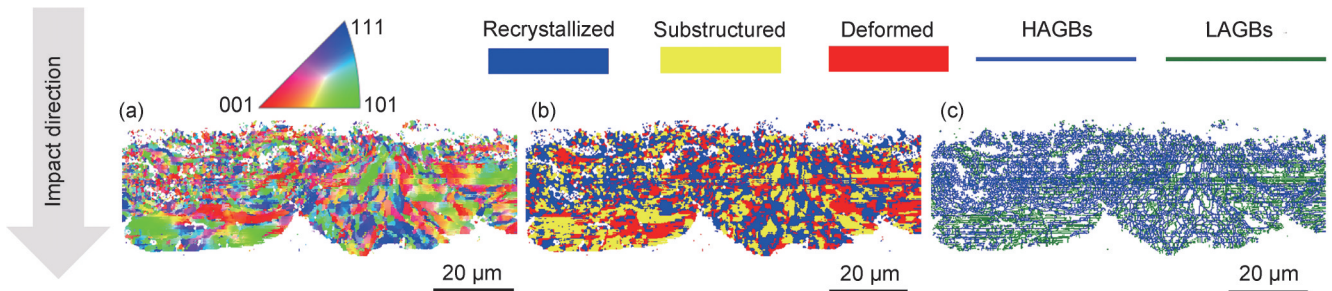


图4 1100 °C制备的Cr涂层截面EBSD分析

(a)IPF图;(b)晶粒取向差分布图;(c)晶界分布图

Fig.4 EBSD analysis of Cr coatings cross-section at 1100 °C

(a)IPF map;(b)GOS map;(c)grain boundary distribution map

2.2 基体及涂层纳米硬度

基体及涂层纳米硬度的表征均在喷涂温度为1100 °C的样品上进行。对在涂层与基体结合界面处以及远离结合界面处的纳米硬度分布进行表征发现,远离结合界面处的基体纳米硬度为3.49 GPa,而靠近结合界面处的纳米硬度值则达到5.75 GPa,增幅高达64.8%。结合图2(b)中显示的不规则结合界面,可以推断,在粒子沉积过程中粒子与基体经历显著的协同塑性变形,导致基体产生明显的加工硬化现象。

图5为沿涂层成形方向的纳米硬度分布。可以发现,Cr粒子的平均纳米硬度为4.52 GPa,涂层的纳米硬度沿涂层成形方向呈梯度分布,且均高于未变形粒

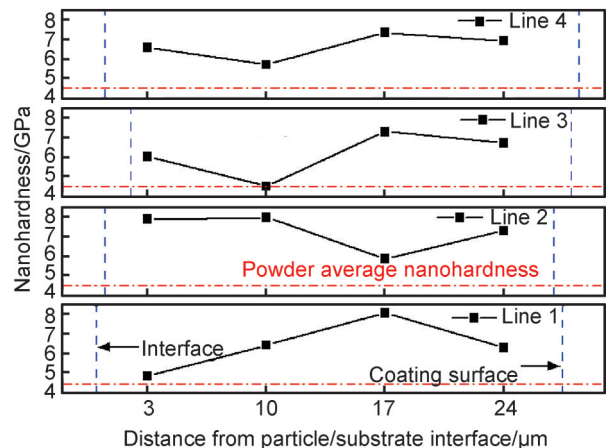


图5 Cr涂层的纳米硬度分布(单个变形粒子)

Fig.5 Nanohardness distributions of Cr coatings (single splat)

子^[33]。对靠近涂层与基体结合界面处的纳米硬度进行分析可知,Line 1 在该处的纳米硬度为 4.94 GPa,接近未变形粒子,而 Line 2、Line 3 以及 Line 4 在该处的纳米硬度分别为 7.90、6.01 GPa 以及 6.57 GPa,均明显高于未变形粒子。在粒子与基体碰撞过程中发生协同塑性变形,但粒子与基体结合界面处的塑性变形程度不一致,导致加工硬化程度不一致。根据 Zhang 等^[34]的模拟结果,结合界面两侧发生的塑性变形程度较大,而中间底部的塑性变形程度较小,这在已发表文献中也得到了实验验证^[4,35-36]。Line 1、Line 2、Line 3 以及 Line 4 靠近涂层表面处的纳米硬度分别为 6.39、7.33、6.77 GPa 以及 6.92 GPa,均显著高于未变形粒子,较未变形粒子提升了 41.37%~62.17%,该结果与图 4(a)的晶粒大小分布相对应。

2.3 冷喷涂 Cr 涂层在 304 不锈钢上的成形机制

结合涂层的微观形貌与纳米硬度分布,对冷喷涂 Cr 涂层在 304 不锈钢基体上的沉积机制进行阐释,如图 6 所示。该机制可划分为 6 个阶段(注:本机制不涉及 Cr 粒子在已沉积涂层上的沉积过程):(1)冷喷涂前未对基体进行喷砂,因而基体表面仍存在氧化膜(图 6(a))。(2)由于氧化膜的作用,首层与基体发生碰撞的粒子

难以与基体产生结合,主要起到破碎氧化膜的作用,导致大部分粒子反弹,仅有少部分粒子与裸露出的新鲜金属结合。同时,在碰撞过程中基体发生塑性变形,并伴随一定程度的加工硬化,使原本平整的表面在微观尺度上逐渐呈现出不均匀的凹凸特征^[37]。该阶段 Cr 粒子与基体之间的相互作用效果类似于喷砂(图 6(b))。(3)随着氧化膜被有效破碎,后续粒子与裸露出的新鲜金属之间通过协同塑性变形实现结合,从而逐步形成涂层^[38],在本阶段,粒子与基体之间的结合基本完成(图 6(c))。(4)受冷喷涂固有特性的影响,粒子与基体的结合界面处会发生较大的塑性变形,而粒子上半部分则基本保持半球形态。由于粒子在基体上的分布呈随机性,大部分后续粒子将与已沉积粒子的侧面发生碰撞。根据 Zhou 等^[39]的研究,这种碰撞方式增加了粒子的反弹倾向,从而阻碍其在涂层上的继续沉积,并对已沉积涂层产生喷丸强化的作用。此外,Vaz 等^[40]在冷喷涂增材制造“垂直墙体”过程中为提高沉积效率,实时调整喷涂角度,保证喷枪与喷涂面为 90°,该策略与本分析相吻合(图 6(d))。(5)随着喷涂过程的持续,已沉积的粒子在喷丸效应作用下逐渐演变为凹陷状形态(图 6(e))^[41]。(6)当涂层表面发

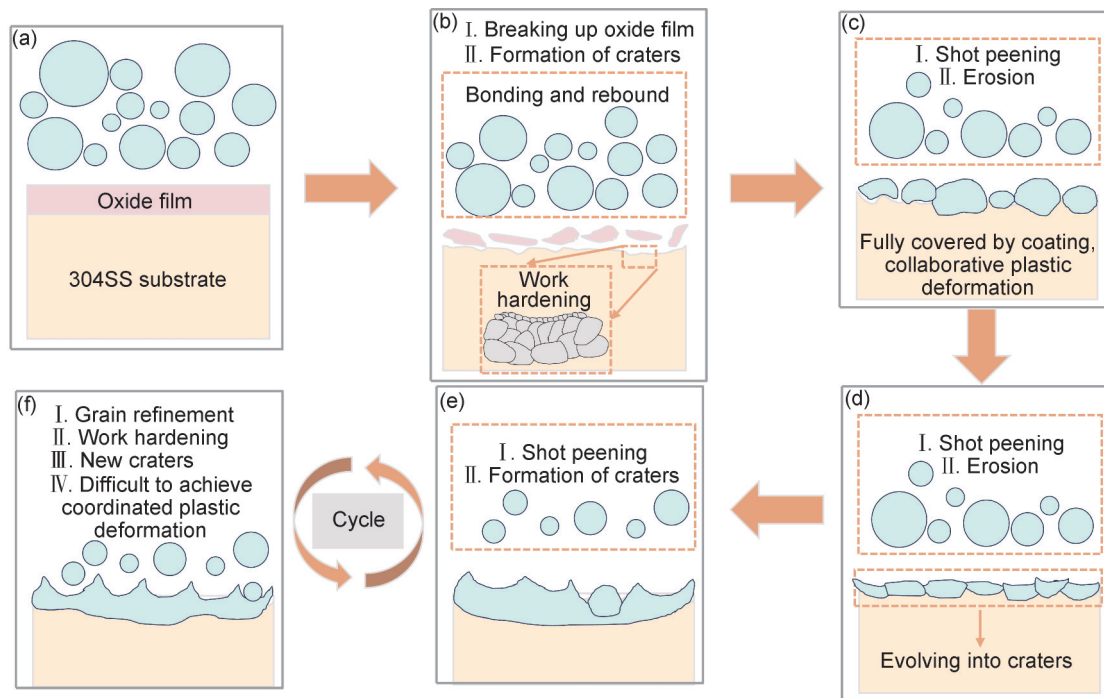


图 6 304 不锈钢基体上 Cr 涂层的成形机制

(a)粒子碰撞基体前状态;(b)粒子与基体发生碰撞,基体氧化膜破碎;(c)粒子与基体相结合;
(d)已沉积涂层表面逐渐向凹坑演变;(e)已沉积涂层表面演变为凹坑;(f)已沉积涂层表面演变为新的凹坑并与图 6(e)构成循环

Fig.6 Forming mechanism of Cr coatings on 304 stainless steel substrate

(a)state of particles prior to impact substrate;(b)particles impact substrate,causing rupture of substrate's oxide film;(c)particles bond with substrate;
(d)surface of deposited coating gradually evolving into a cratered morphology;(e)surface of deposited coating further evolving into craters;
(f)new craters form on deposited coating surface,establishing a cyclic process with stage Fig.6(e)

展为凹陷状态后,由于喷丸强化效应,涂层近表面的晶粒不断细化,导致该区域硬度显著提高(图6(f))。此时,硬脆的Cr粒子与经过加工硬化的Cr涂层发生碰撞,难以实现协同塑性变形,部分粒子因内聚强度不足而破碎,大部分粒子则发生反弹难以沉积。随着喷涂的持续进行,原有凹陷逐步演变为新的凹陷,晶粒细化与加工硬化现象并存。需要指出的是,虽然部分粒子以嵌入形式沉积于涂层内部,但这种结合较为脆弱,难以承载有效载荷。在冷喷涂过程中,本阶段与图6(e)阶段循环往复出现。

3 结论

(1)电镀法制备的Cr涂层内部存在大量纵向裂纹,相比之下,冷喷涂法制备的Cr涂层内部较为致密,且涂层与基体之间的结合界面无缺陷,展现出作为电镀替代工艺的优势。

(2)冷喷涂制备的Cr涂层表面普遍存在大量凹坑,且近表面区域形成细小的等轴晶结构,该区域的纳米硬度较未变形粒子提高了41.37%~62.17%,表明喷丸强化效应显著,该过程抑制了后续粒子的沉积。

(3)Cr涂层在304不锈钢基体上的沉积成形机制主要包括:基体氧化膜的破碎、首层涂层的形成以及在喷丸强化作用下涂层表面微观形貌的演变过程。

致谢:感谢德国汉堡赫尔穆特-施密特大学/德国联邦国防军大学材料技术研究所的T. Klassen教授和F. Gaertner研究员对喷涂实验的支持。

参考文献

- [1] BISCHOFF J, DELAFOY C, VAUGLIN C, et al. AREVA NP's enhanced accident-tolerant fuel developments: focus on Cr-coated M5 cladding [J]. Nuclear Engineering and Technology, 2018, 50(2):223-228.
- [2] BRACHET J, IDARRAGA-TRUJILLO I, FLEM M L, et al. Early studies on Cr-coated zircaloy-4 as enhanced accident tolerant nuclear fuel claddings for light water reactors[J]. Journal of Nuclear Materials, 2019, 517:268-285.
- [3] CHEN Q S, LIU C H, ZHANG R Q, et al. Microstructure and high-temperature steam oxidation properties of thick Cr coatings prepared by magnetron sputtering for accident tolerant fuel claddings: the role of bias in the deposition process[J]. Corrosion Science, 2020, 165:108378.
- [4] FAZI A, STILLER K, ANDRÉN H, et al. Cold sprayed Cr-coating on optimized ZIRLO™ claddings: the Cr/Zr interface and its microstructural and chemical evolution after autoclave corrosion testing[J]. Journal of Nuclear Materials, 2022, 560:153505.
- [5] HAN Z, WANG Z, WANG Z, et al. Tailored high-temperature corrosion behavior of Cr coatings using high power impulse magnetron sputtering on ZIRLO alloys for accident-tolerant fuel application[J]. Surface and Coatings Technology, 2024, 488:130941.
- [6] LIANG A, WANG Y, WANG F, et al. Fantastic behavior of near zero wear of Cr-based coatings [J]. Materials Letters, 2022, 319:132228.
- [7] XIANG Y, ZHAO S, LIU C, et al. Effect of long-term aging treatment on the structure and oxidation resistance of Cr coatings under high-temperature steam [J]. Corrosion Science, 2023, 212:110923.
- [8] PINHEIRO X L, OLIVEIRA K, SANTOS J, et al. The combination of electrodeposited chromium (III) and PVD as an industrial viable solution for the replacement of electrodeposited chromium (VI) [J]. Process Safety and Environmental Protection, 2024, 182:727-739.
- [9] LEIMBACH M, TSCHAAR C, ZAPF D, et al. Relation between color and surface morphology of electrodeposited chromium for decorative applications [J]. Journal of the Electrochemical Society, 2019, 166(6):D205-D211.
- [10] CHANDRASEKAR M S, PUSHPAVANAM M. Pulse and pulse reverse plating-conceptual, advantages and applications [J]. Electrochimica Acta, 2008, 53(8):3313-3322.
- [11] IMAZ N, OSTRÁ M, VIDAL M, et al. Corrosion behaviour of chromium coatings obtained by direct and reverse pulse plating electrodeposition in NaCl aqueous solution [J]. Corrosion Science, 2014, 78:251-259.
- [12] YEO S, KIM J H, YUN H S. Effect of pulse current and coating thickness on the microstructure and FCCI resistance of electroplated chromium on HT9 steel cladding [J]. Surface and Coatings Technology, 2020, 389:125652.
- [13] YEO S, YUN H S, KIM J H, et al. Direct and pulse electroplating effects on the diffusion barrier property of plasma-nitrided Cr coatings on HT9 steel [J]. Journal of Nuclear Materials, 2023, 574:154218.
- [14] LI Q, SONG P, ZHANG R, et al. Oxidation behavior and Cr-Zr diffusion of Cr coatings prepared by atmospheric plasma spraying on zircaloy-4 cladding in steam at 1300 °C [J]. Corrosion Science, 2022, 203:110378.
- [15] LI N, CHEN L, CHAI L, et al. A novel plasma-sprayed Cr/FeCrAl dual-layer coating on Zr alloy for potential high-temperature applications [J]. Journal of Materials Research and Technology, 2024, 30:5569-5581.
- [16] 严俊, 廖业宏, 彭振驯, 等. Cr涂层钎合金事故容错燃料包壳材料研究进展 [J]. 表面技术, 2023, 52(12):206-224.
YAN J, LIAO Y H, PENG Z X, et al. Review on Cr-coated zirconium alloy cladding for accident tolerant fuel [J]. Surface Technology, 2023, 52(12):206-224.
- [17] 雷一明. 几种事故容错燃料包壳涂层的设计、制备与性能研究 [D]. 合肥:中国科学技术大学, 2021.
LEI Y M. Design, synthesis and properties of protective coatings for accident tolerant fuels [D]. Hefei: University of Science and Technology of China, 2021.
- [18] TAILOR S, MODI A. Behavior of high-velocity oxygen fuel sprayed chromium-coating on zircaloy-4 fuel cladding under loss-of-coolant accident conditions [J]. Materials Letters, 2024, 377:

- 137431.
- [19] KIM H, KIM I, JUNG Y, et al. Adhesion property and high-temperature oxidation behavior of Cr-coated zircaloy-4 cladding tube prepared by 3D laser coating[J]. *Journal of Nuclear Materials*, 2015, 465: 531-539.
- [20] QIU X, QI L, TANG J, et al. A viable approach to repair neutron shielding B₄C/6061 Al composite sheets through cold spray and hot rolling co-treatment[J]. *Journal of Materials Science & Technology*, 2022, 106: 173-182.
- [21] YIN S, FAN N, HUANG C, et al. Towards high-strength cold spray additive manufactured metals: methods, mechanisms, and properties[J]. *Journal of Materials Science & Technology*, 2024, 170(3): 47-64.
- [22] WU D, ZHANG J, SU Y, et al. Effect of powder feeding rate and size on critical velocity and mechanical properties of cold sprayed Al₂O₃/2024 deposit[J]. *Chinese Journal of Aeronautics*, 2024, 37(12): 544-559.
- [23] WU D, ZHANG J, LI W, et al. Morphology of ceramic regulates the deposition behavior and mechanical properties of cold spray additive manufactured Al₂O₃/2024 aluminum matrix composites[J]. *Materials Characterization*, 2024, 215: 114197.
- [24] WAN W, LI W, WU D, et al. New insights into the effects of powder injector inner diameter and overhang length on particle accelerating behavior in cold spray additive manufacturing by numerical simulation[J]. *Surface and Coatings Technology*, 2022, 444: 128670.
- [25] WAN W, LI W, WU D, et al. 3D analysis of gas flow behavior and particle acceleration characteristics in cold spray additive manufacturing based on non-axisymmetric numerical models[J]. *Journal of Materials Research and Technology*, 2024, 29: 1335-1349.
- [26] 黄春杰, 殷硕, 李文亚, 等. 冷喷涂技术及其系统的研究现状与展望[J]. *表面技术*, 2021, 50(7): 1-23.
HUANG C J, YIN S, LI W Y, et al. Cold spray technology and its system: research status and prospect[J]. *Surface Technology*, 2021, 50(7): 1-23.
- [27] YEOM H, JOHNSON G, MAIER B, et al. High temperature oxidation of cold spray Cr-coated accident tolerant zirconium-alloy cladding with Nb diffusion barrier layer[J]. *Journal of Nuclear Materials*, 2024, 588: 154822.
- [28] UMRETIYA R V, WORKU M, ABOUELELLA H, et al. Hydrothermal corrosion of PVD and cold spray Cr-coatings on zircaloy-4 in hydrogenated and oxygenated LWR coolant environments[J]. *Nuclear Materials and Energy*, 2023, 37: 101519.
- [29] FAZI A, SATTARI M, STILLER K, et al. Performance and evolution of cold spray Cr-coated optimized ZIRLO™ claddings under simulated loss-of-coolant accident conditions[J]. *Journal of Nuclear Materials*, 2023, 576: 154268.
- [30] LI W, XUE N, SHAO L, et al. Effects of spraying parameters and heat treatment temperature on microstructure and properties of single-pass and single-layer cold-sprayed Cu coatings on Al alloy substrate[J]. *Surface and Coatings Technology*, 2024, 490: 131184.
- [31] 黄春杰, 张正茂, 雒晓涛, 等. 基于替代电镀硬铬的WC增强金属复合涂层疲劳性能的研究现状[J]. *精密成形工程*, 2024, 16(7): 205-214.
HUANG C J, ZHANG Z M, LUO X T, et al. Research status of fatigue properties of WC reinforced metal composite coatings based on alternative electroplated hard chrome[J]. *Journal of Net-shape Forming Engineering*, 2024, 16(7): 205-214.
- [32] WANG H, YAO H, ZHANG M, et al. Surface nanocrystallization treatment of AZ91D magnesium alloy by cold spraying shot peening process[J]. *Surface and Coatings Technology*, 2019, 374: 485-492.
- [33] ALAKIOZIDIS I, HUNT C, SMITH A D, et al. Microstructure and mechanical performance of cold spray Cr coatings[J]. *Journal of Nuclear Materials*, 2025, 604: 155492.
- [34] ZHANG Z, LIU Z, ZHAO J, et al. Numerical analysis of residual stresses induced by cold spray fabricating cBN-reinforced Ni matrix composites[J]. *Surface and Coatings Technology*, 2023, 467: 129672.
- [35] FAZI A, ABOULFADL H, IYER A H S, et al. Characterization of as-deposited cold sprayed Cr-coating on optimized ZIRLO™ claddings[J]. *Journal of Nuclear Materials*, 2021, 549: 152892.
- [36] DABNEY T, SASIDHAR K N, WILLING E, et al. Microstructural evolution in ion irradiated cold spray Cr coated Zr-alloy[J]. *Journal of Nuclear Materials*, 2025, 606: 155652.
- [37] BRUERA A, PUDDU P, THEIMER S, et al. Adhesion of cold sprayed soft coatings: effect of substrate roughness and hardness[J]. *Surface and Coatings Technology*, 2023, 466: 129651.
- [38] ICHIKAWA Y, OGAWA K. Effect of substrate surface oxide film thickness on deposition behavior and deposition efficiency in the cold spray process[J]. *Journal of Thermal Spray Technology*, 2015, 24(7): 1269-1276.
- [39] ZHOU H, LI Z, WEI X, et al. Effect of particle deposition location on interface bonding during cold spraying[J]. *Powder Technology*, 2024, 448: 120355.
- [40] VAZ R F, ALBALADEJO-FUENTES V, SANCHEZ J, et al. Metal knitting: a new strategy for cold gas spray additive manufacturing[J]. *Materials*, 2022, 15(19): 6785.
- [41] GAO P, LI C, YANG G, et al. Influence of substrate hardness transition on built-up of nanostructured WC-12Co by cold spraying[J]. *Applied Surface Science*, 2010, 256(7): 2263-2268.

基金项目: 核电安全技术与装备全国重点实验室开放基金资助(SKL-2024-TS-01); 西北工业大学凝固技术全国重点实验室课题资助(2025-DXZX-ZC-02); 中央高校基本科研业务费专项(G2024KY05107)

收稿日期: 2025-03-11; 录用日期: 2025-05-07

通讯作者: 黄春杰(1988—), 男, 教授, 博士生导师, 博士, 研究方向为喷涂及焊接等金属连接与增材/修复技术, 联系地址: 陕西省西安市友谊西路127号西北工业大学陕西省摩擦焊接工程技术重点实验室(710072), E-mail: huangc@nwpu.edu.cn

(本文责编: 王 晶)